

Synthesis and applications of functionalized silsesquioxane polymers attached to organic and inorganic matrices*

Yoshitaka Gushikem[‡], Edilson V. Benvenutti, and Yuriy V. Kholin

Institute of Chemistry, Campinas State University, CP 6154, 13084-971, Campinas, SP, Brazil; Institute of Chemistry, Rio Grande do Sul National University, 91501-970, Porto Alegre, RS, Brazil; V. N. Karazin Kharkiv National University, 4 Svoboda Square, Kharkiv, 61077, Ukraine

Abstract: Organofunctionalized silsesquioxane polymers obtained in a water-soluble form can be used to coat various substrates such as SiO₂, SiO₂/Al₂O₃, Al₂O₃, cellulose/Al₂O₃, and graphite or, when obtained in a water-insoluble form, can be used directly. These organofunctionalized silsesquioxanes can also be attached to poly(dimethylsiloxane) (PDMS) polymers. The functional groups constituted by neutral amine groups or cationic groups (pyridinium, 3- and 4-picolinium, or 1,4-diazabicyclo[2.2.2]octane (DABCO), mono- or -dicationic) have relatively high affinity for metal ion in ethanol solutions, as shown by their stability constants. Materials containing attached cationic functional groups have also been efficiently used to immobilize various electroactive species and to construct electrochemical sensors for analytical applications. This work discusses the preparation of silsesquioxane derivatives, their characterization as prepared and when dispersed on several substrates, and comments on some applications of these materials, with an emphasis on the metal adsorption process and manufacture of electrochemical sensors.

Keywords: silsesquioxane polymers; organofunctionalized silsesquioxane polymers; sol-gel; adsorption; electrochemical sensors; chemically modified surfaces.

INTRODUCTION

Many organofunctional groups, such as alkylammonium, imidazolium, or pyridinium groups, have been bonded to silica matrix in recent years for applications in ion-exchange processes. Most of these organofunctional silica materials have been prepared by the sol-gel processing method. Materials incorporating these organic substituent groups, covalently linked to the silica matrix, combine the physical properties of a glass, such as thermal stability and rigidity with the exchange properties of the organofunctional groups [1–5].

Covalently attaching organofunctional groups onto substrates of porous materials such as silica is another procedure to obtain pressure-resistant materials for use as silica-based phases for anion-exchange chromatography [6,7], as adsorbent for biological materials, and for disinfection of drinking water [8,9].

*Paper based on a presentation at the International Conference on Modern Physical Chemistry for Advanced Materials (MPC '07), 26–30 June 2007, Kharkiv, Ukraine. Other presentations are published in this issue, pp. 1365–1630.

[‡]Corresponding author

In recent years, attention has also been devoted to development of new sensing electrodes for detection of ionic compounds in water. Silica modified by grafting reactions with glycidyltrimethylammonium chloride has been prepared to study anion-exchange affinity for different anions by impedance measurements [10]. Films of quaternary amines or pyridinium anion organofunctional groups have been dispersed on electrode surfaces to investigate anion-exchange property by electroanalytical techniques [11,12]. Films dispersed on mesoporous silica surfaces presenting long-range order porosity, have been prepared by viewing applications such as membranes and sensors where powdered samples cannot be used and the thin film geometry is essential [13].

Other classes of materials-denominated, organic-inorganic hybrid mesoporous anion-exchange resins have been prepared using mesoporous silica and organosilica materials as support for specific applications for perchlorate adsorption [14]. Belonging to this class of materials, nanocomposites of SiO_2 /poly(methylacrylate) for applications in chemical separation, electrochemical sensing, and water treatment have been described [15].

Adsorption on substrates modified with organofunctionalized silica from nonaqueous solvents has been the subject of investigation aimed at development of materials presenting high capacity and selective adsorption of several metal ions. Tests carried out with these materials have shown high affinity in removing Cu(II), Fe(III), Co(II), Cu(II), Zn(II), Cd(II), and Hg(II) from ethanol solutions [16–20]

Considering the high potential use of these chemically modified substrates in adsorption processes, in fabricating electrochemical sensors, for high-performance liquid chromatography (HPLC) packing materials, in catalysis, and for many other uses, in this paper we describe the preparation, characterization, and use of some organofunctionalized silane groups attached on several substrates. A particular emphasis is given to adsorption of metal ions from ethanol solutions, which coincides with present discussions on the use of ethanol as fuel. As ethanol is widely used in Brazil as a fuel and, considering the limits of metal content allowed according to the Brazilian National Petroleum Agency norms [21], development of a membrane to efficiently retain trace amounts of metals is of fundamental importance.

SYNTHESES OF THE MATERIALS AND THEIR CHARACTERISTICS

The silsesquioxane derivatives are prepared mainly by the sol-gel processing method, considering that this procedure allows the obtainment of products with high purity and with reproducibility [22]. A general and schematic procedure to prepare derivatives containing pyridinium, picolinium, and 1,4-diazabicyclo[2.2.2]octane (DABCO) cationic group is shown in Scheme 1:

The procedures to obtain all materials are very simple and consist basically in acid prehydrolysis of tetraethyl orthosilicate (TEOS), in ethanol solution, in water presence, followed by the addition of the organic group of interest: pyridine, 3-picoline, 4-picoline, or 1,4-diazabicyclo[2.2.2]octane.

The polymers 3-*n*-propylpyridinium chloride silsesquioxane, designated as SiPy^+Cl^- , and 3-*n*-propyl-1-azonia-4-azabicyclo[2.2.2]octane chloride silsesquioxane, designated as SiDb^+Cl^- , are soluble in water and thus, they are more conveniently used by supporting them on several surfaces, such as SiO_2 , $\text{SiO}_2/\text{Al}_2\text{O}_3$ [23–25], Al_2O_3 [26], graphite [27], cellulose/ Al_2O_3 (cellulose coated with thin film of hydrated aluminum oxide) [28], and a mesoporous aluminum phosphate surface [29].

In the particular case of SiDb^+Cl^- , the material prepared with a lower content of the functional organic cationic groups (i.e., when the DABCO content is <25 mol % in the material prepared) can lead to formation of a water-insoluble polymer [30]. In this case, SiDb^+Cl^- can be used as prepared. $\text{Si3Pic}^+\text{Cl}^-$ and $\text{Si4Pic}^+\text{Cl}^-$ were always obtained as water-insoluble products and then used directly.

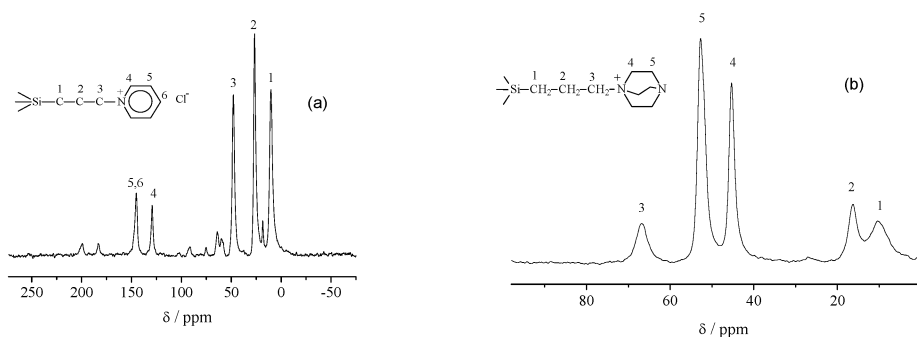
Structural information on these materials was obtained by several techniques. In particular, due to the amorphous nature of the solids, solid-state NMR technique has been of fundamental importance.

Table 1 Chemical analysis results (CHN), ionized chloride content and solubility in water for SiPy⁺Cl⁻ and SiDb⁺Cl⁻.

Materials	C, wt %	H, wt %	N, wt %	SiO ₂ , wt %	Cl ⁻ , mmol g ⁻¹	Solubility, g/100 ml
SiPy ⁺ Cl ⁻ ^a	29.9	4.9	4.0	57.5	3.0	~20
SiDb ⁺ Cl ⁻ ^b	21.1	4.6	4.9	62.2	2.0	1.2



Figure 1 shows the ¹³C solid-state NMR spectra for both polymers, SiPy⁺Cl⁻ (2a) [28] and SiDb⁺Cl⁻ (2b) [31].

**Fig. 1** Solid-state ¹³C NMR spectra of: (a) SiPy⁺Cl⁻, (b) SiDb⁺Cl⁻.

The soluble polymers can be directly dispersed on a surface of SiO₂, graphite and a surface previously coated with thin a film of Al₂O₃. The good adherence of the substrates coated onto Al₂O₃ is due to the high affinity of the AlOH group on the alumina surface by the silanol group, SiOH, forming the stable Al–O–Si bond.

Figure 2 shows a typical ²⁷Al NMR spectrum obtained upon coating the SiO₂/Al₂O₃ surface with the polymer SiPy⁺Cl⁻. The relative intensity of the peak at 2 ppm (Fig. 2a) due to Al₆ (hexacoordinated) in comparison with Al₄ (tetraordinated) decreases after reacting with SiPy⁺Cl⁻ (Fig. 2b) [25]. The observed change is suggested to be due to the changing of coordination from six- to four-fold upon contact with SiPy⁺Cl⁻ and formation of a Si–O–Al bonding [32–34]. However, the exact mechanism on how such reaction occurs on the surface was not investigated in detail.

The adherence occurs on a graphite surface, but the interaction presumably is of an electrostatic nature. In this case, the procedure is very simple and consists in immersing graphite (as a disk or rod) into a dilute solution of the polymer SiPy⁺Cl⁻, and after 30 min of this contact, removing the graphite and allowing the water to evaporate, at room temperature from the modified graphite surface. The resulting material is designated as C/SiPy⁺Cl⁻.

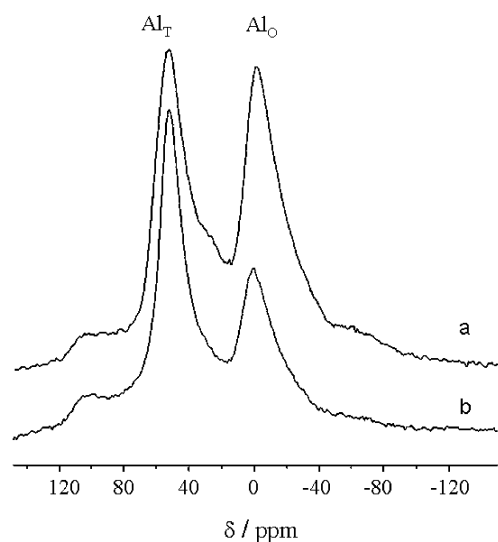


Fig. 2 MAS ^{27}Al NMR spectra of: (a) $\text{SiO}_2/\text{Al}_2\text{O}_3$, (b) $\text{SiO}_2/\text{Al}_2\text{O}_3/\text{SiPy}^+\text{Cl}^-$.

Polymers containing the 3- and 4-picolinium group are obtained as water-insoluble materials, and, thus, they are used as prepared [35]. Table 2 presents the chemical analyses results for 3-*n*-propyl-3-picolinium chloride silsesquioxane and 3-*n*-propyl-4-picolinium chloride silsesquioxane, designated as $\text{Si3Pic}^+\text{Cl}^-$ and $\text{Si4Pic}^+\text{Cl}^-$, respectively. Figure 3 shows the solid-state ^{13}C NMR of $\text{Si3Pic}^+\text{Cl}^-$ and $\text{Si4Pic}^+\text{Cl}^-$.

Table 2 Chemical analysis results (CHN) and ionized chloride for $\text{Si3Pic}^+\text{Cl}^-$ and $\text{Si4Pic}^+\text{Cl}^-$.

Materials	C, wt %	H, wt %	N, wt %	SiO_2 , wt %	Cl^- , mmol g^{-1}
$\text{Si3Pic}^+\text{Cl}^-$	23.0	4.5	6.8	63.0	1.91
$\text{Si4Pic}^+\text{Cl}^-$	21.0	4.2	2.2	66.0	1.46

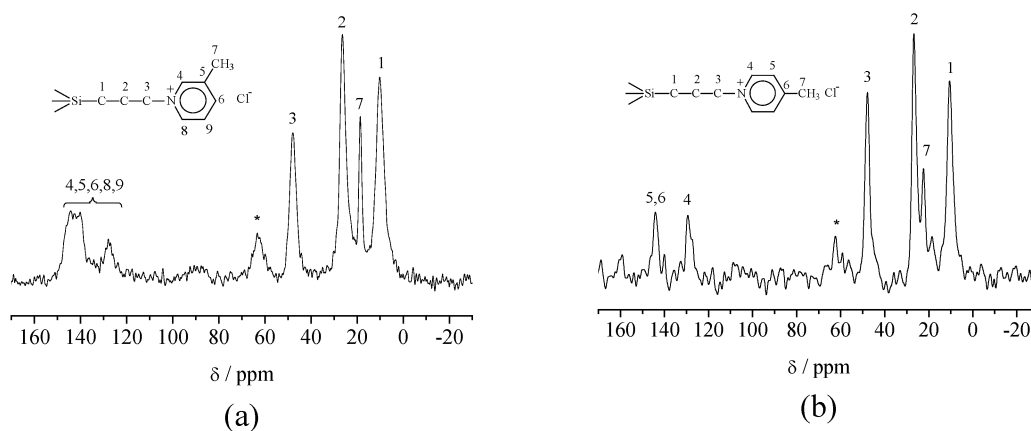
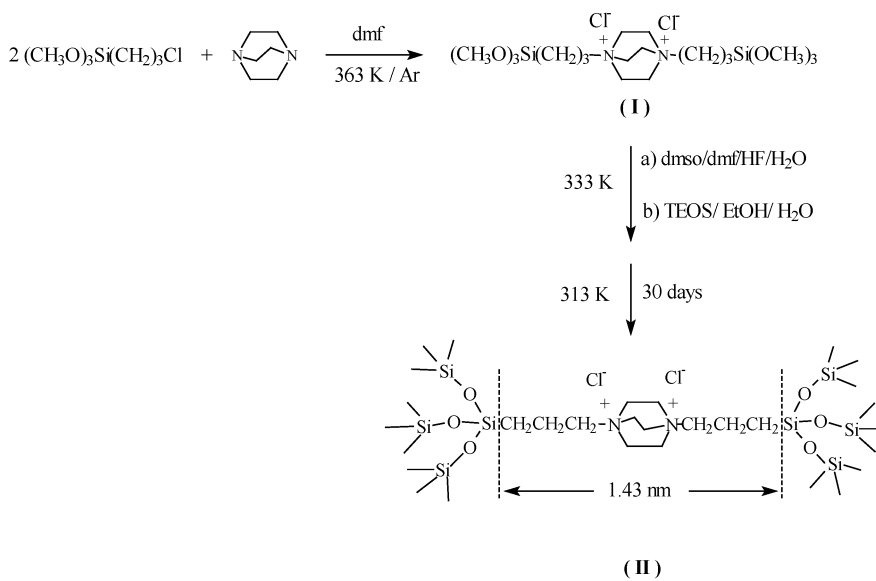


Fig. 3 Solid-state ^{13}C NMR spectra of (a) $\text{Si3Pic}^+\text{Cl}^-$, (b) $\text{Si4Pic}^+\text{Cl}^-$. (*) unreacted chloropropyl group, $\equiv\text{Si}(\text{CH}_2)_3\text{Cl}$.

The synthesis of material containing the bridged functional group $-\overset{+}{N}(\text{CH}_2\text{CH}_2)_3\overset{+}{N}-$, is carried out in two steps (see Scheme 2): (a) DABCO is reacted with 3-chloropropyltrimethoxysilane in dimethylformamide (DMF) under an argon atmosphere at a temperature of 363 K. The white solid is 1,4-bis-(3-trimethoxysilylpropyl)diazoniabicyclo [2.2.2]octane chloride (I). (b) The precursor (I) is now reacted with TEOS in a mixture of solvents dimethyl sulfoxide (DMSO)/DMF/HF/H₂O. The mixture is allowed to rest for 30 days at controlled temperature of 313 K for gelation [36].



Scheme 2 Preparation of $\text{SiO}_2/\text{-}\overset{+}{N}(\text{CH}_2\text{CH}_2)_3\overset{+}{N}\text{-}/\text{SiO}_2$ by the sol-gel processing method.

The inorganic/organic hybrid (II) prepared with different contents of DABCO group was submitted to elemental analyses, and the results are reported in Table 3.

Table 3 C,N analyses for hybrid material (II).

Samples	C, wt %	N, wt %	N/C mole ratios
D1	3.89 (3.24)	0.66 (0.47)	0.15
D2	4.06 (3.38)	0.76 (0.54)	0.16
D3	4.61 (3.84)	1.00 (0.71)	0.18

In parenthesis: mmol g^{-1} ; expected N/C mole ratio = 0.17

The specific surface areas and the pore diameters determined by small-angle X-ray scattering (SAXS) measurements revealed interesting results which deserve some comments.

The specific surface areas, S_{BET} , and the pore diameters values are summarized in Table 4.

Table 4 N₂ adsorption isotherms and SAXS results.

Samples	S _{BET} , m ² g ⁻¹	Pore diameter, nm
D1	570 ± 25	1.6 ± 0.1
D2	290 ± 26	1.4 ± 0.1
D3	390 ± 27	1.7 ± 0.01

The surface areas obtained for the three samples reveal that D₁, D₂, and D₃ are very porous, while the diameters of the pores obtained by SAXS technique are very close. It has been proposed that the pore structure of the hybrid material is imposed by the bridged organic group, which has an estimated length of 1.43 nm, as illustrated in Scheme 2. It has already been reported that the length of the bridge chain is related to the average pore size of the hybrid material [37]. Preparation of crystal-like silica-based hybrid materials with control of the anisotropic organization of the nanostructure, by using a neutral bridged organic group, has also been reported [38–40].

While the polymer SiDb⁺Cl⁻ is amorphous, [(SiO₂)₂Db²⁺]Cl₂ is structurally ordered with pore diameters close to 1.5 nm. The high specific surface area is clearly related to the existence of pores whose average diameters are determined by the length of the -(CH₂)₃⁺N(CH₂)₂N⁺(CH₂)₃- chain. Due to this porous character of the material, the anionic complex [Fe(CN)₆]⁴⁻ is adsorbed and confined in these pores. Cyclic voltammetry experiments carried out by changing the potential between -0.2 and 0.8 V are shown in Fig. 4 [36]. The experiments were carried out in 1 M KCl supporting electrolyte solution at a scan rate of 1 mV s⁻¹.

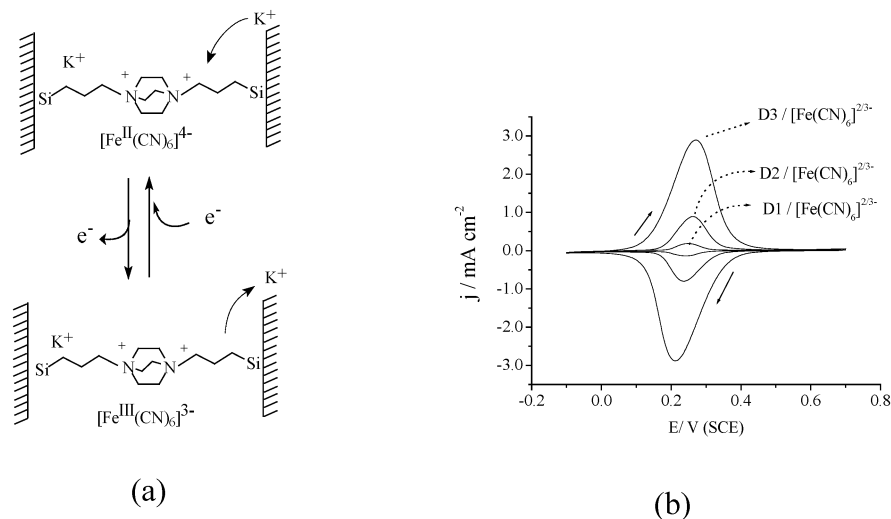


Fig. 4 (a) Redox process of [Fe(CN)₆]^{4-/3-} confined in the pores of the matrix, (b) cyclic voltammetric curves obtained for D1, D2, and D3 matrices.

During the redox process, diffusion of K⁺ ions into and out of the cavity is not affected because the pore size is very large compared to the hydrated ionic radius of the cation (i.e., 0.24 nm). The interaction of the hexacyanoferrate complex through an electrostatic interaction with the fixed doubly charged cationic DABCO ion is sufficiently strong to keep the electroactive species confined in the pores. Experiments consisting of cycling the potential for long times and measuring the cathodic and

diacetate as catalyst; (b): a fine powder of the product obtained is immersed in a dry ethanol solution of pyridine resulting in a translucent yellowish elastomeric material.

According to Scheme 3, the ending $-\text{Si}(\text{CH}_3)_2\text{OH}$ groups of PDMS react with the $(\text{CH}_3\text{O})_2\text{Si}(\text{CH}_2)_3\text{Py}^+\text{Cl}^-$, forming a cluster of propylpyridinium silsesquioxane groups, while reactions of two or more ending $-\text{Si}(\text{CH}_3)_2\text{OH}$ groups lengthen the PDMS chain.

Figure 6 shows the ^{13}C NMR spectrum of the material $\text{PDMS}/\text{SiPy}^+\text{Cl}^-$. The peaks assigned to C_1 (10 ppm), C_2 (26 ppm), C_3 (46 ppm), C_α (130 ppm) and $\text{C}_{\beta,\gamma}$ (146 ppm) clearly show that the $-(\text{CH}_2)_3\text{Py}^+\text{Cl}^-$ is formed on the surface. The most intense peak C_4 (1 ppm) is due to the $-\text{CH}_3$ groups of the PDMS chain [41].

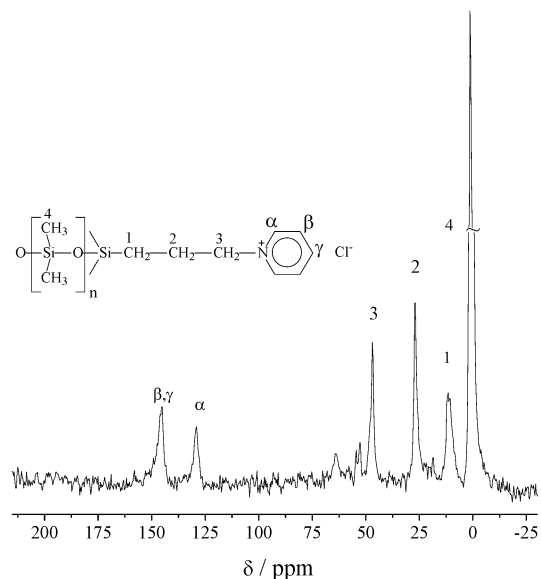


Fig. 6 Solid-state ^{13}C NMR spectrum of $\text{PDMS}/\text{SiPy}^+\text{Cl}^-$.

A typical ^{29}Si NMR spectrum of $\text{PDMS}/\text{Py}^+\text{Cl}^-$, presented in Fig. 7, shows the signal at -68 ppm associated to the **Si** environment in $(\text{SiO})_3\text{Si}-\text{C}$ (T^3) unit of silsesquioxane cluster, present at the nodes of the PDMS network, and a signal at -59 ppm associated with **Si** in $\text{CSi}(\text{OH})(\text{OSi})_2$ (T^2) environment unit, which increases the length of the linear chains between nodes of the polymeric network [25,42].

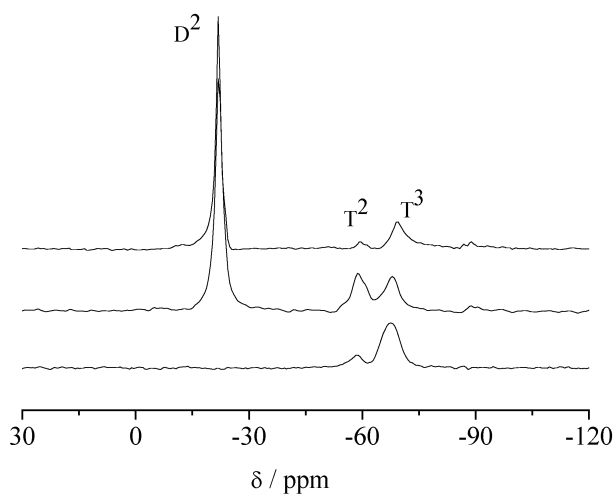


Fig. 7 HPDEC ^{29}Si NMR of (a) Py^+Cl^- , (b) PDMS/Cl, and (c) PDMS/ Py^+Cl^- .

Similarly, the elastomeric PDMS network modified with 3-*n*-propylethylenediamine groups is made reacting $(\text{MeO})_3\text{Si}(\text{CH}_2)_3\text{NH}(\text{CH}_2)_2\text{NH}_2$ with PDMS in tetrahydrofuran as solvent and using tin dibutyldiacetate as catalyst [43]. Figure 8 presents its solid-state ^{13}C NMR spectrum.

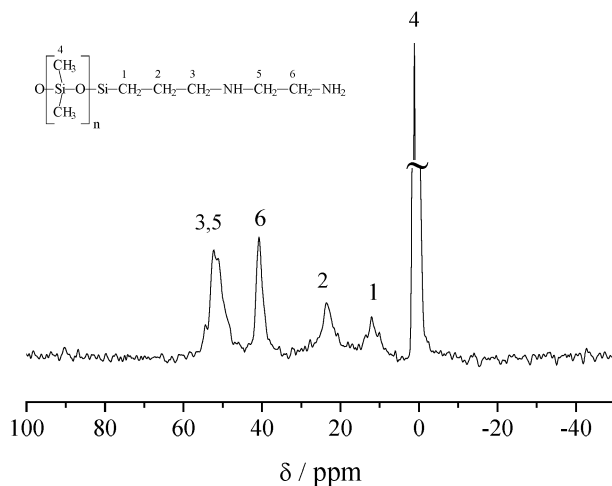
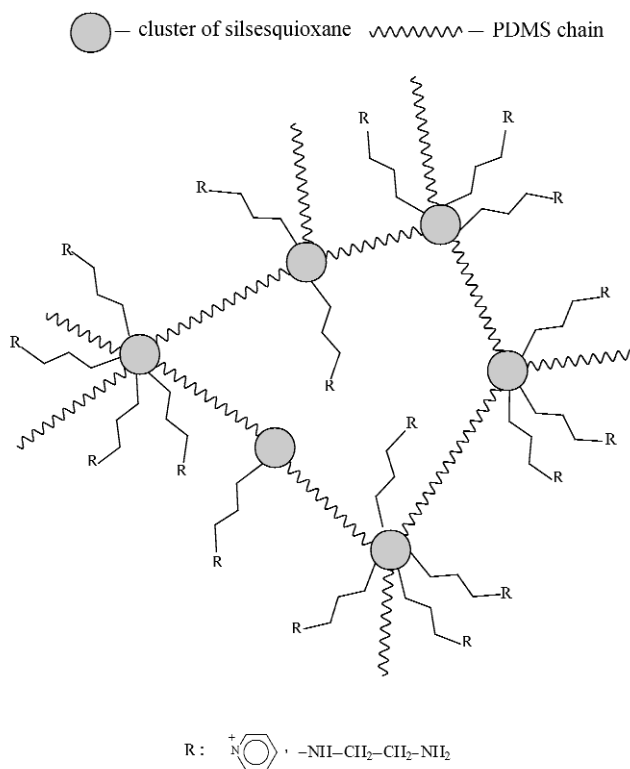


Fig. 8 Solid-state ^{13}C NMR spectrum of PDMS/ethylenediamine.

Scheme 4 shows the idealized structure of chemically modified PDMS with pyridinium ion and ethylenediamine groups.



Scheme 4 Idealized structure of modified PDMS matrix.

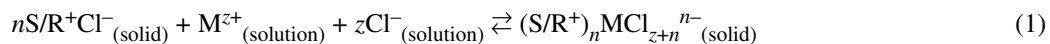
APPLICATION OF THE MATERIALS

Use for anion exchange

The usefulness of thin films of cationic organic groups grafted onto a porous silica surface has been reported for metal complex adsorption [44] and for the anion-exchange process [45,46]. Organofunctionalized silicas containing pyridinium ions, Py^+Cl^- , obtained by the grafting reaction, showed high affinity to ClO_4^- ions. The experimental affinities, in decreasing order for Py^+Cl^- , were: $\text{ClO}_4^- \gg \text{SCN}^- \gg \text{I}^- \gg \text{IO}_4^- \gg \text{Br}^- \gg \text{ClO}_3^- \gg \text{BrO}_3^- \gg \text{IO}_3^-$ [46]. This group dispersed on a silica surface was also used as stationary phase for anion-exchange chromatographic separations [6,7]. More recently, hybrid materials obtained from sol-gel synthesis containing imidazolium derivative species have shown selectivity for perrhenate adsorption [3,14], and 3-*n*-propyl-1-azonia-4-azabicyclo[2.2.2]octane chloride silsesquioxane, SiDb^+Cl^- , or 1,4-bis-(3-trimethoxysilylpropyl)diazonibicyclo[2.2.2]octane chloride silsesquioxane (SiO_2)₂ $\text{Db}^{2+}\text{Cl}_2^-$ sol-gel materials, as thin films dispersed on $\text{SiO}_2/\text{Al}_2\text{O}_3$ surfaces have shown high affinity for Cr(VI) adsorption. The comparison with other adsorbents shows that the SiDb^+Cl^- and (SiO_2)₂ $\text{Db}^{2+}\text{Cl}_2^-$ materials can be successfully employed for removal of Cr(VI) species from aqueous solutions [47,48].

Affinity of the materials coated with cationic functional groups for metal halides

Metal halides, MCl_z , in nonaqueous solutions are adsorbed by the materials by using adsorption isotherms and batch technique, according to the following reaction:



It has been observed that the metal ions M^{z+} diffuse into the solid–solution interface, followed by the anion, i.e., the metal halide is adsorbed on the solid surface as a neutral species, MCl_z , from ethanol solution and adsorbed as MCl_{z+n}^{n-} by reacting with Cl^- at the surface (eq. 1). Experimental evidence is given by the Raman scattering spectra of MCl_z adsorbed on $(SiO_2/SiPy^+)_n MCl_{z+n}^{n-}$, $M = Zn^{2+}$ or Fe^{3+} , as shown in Fig. 9 [49].

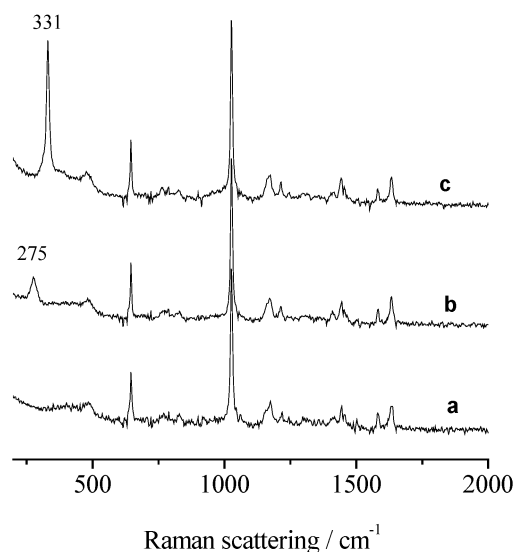


Fig. 9 Raman spectra of: (a) $SiO_2/Al_2O_3/SiPy^+Cl^-$, (b) $[SiO_2/Al_2O_3/SiPy^+]_2ZnCl_4^{2-}$, and (c) $[SiO_2/Al_2O_3/SiPy^+]FeCl_4^-$.

The Raman scattering peaks in Fig. 9b at 275 cm^{-1} and in Fig. 9c at 331 cm^{-1} , are due to the well-known $MCl A_1$ stretching modes of $ZnCl_4^{2-}$ and $FeCl_4^-$ under T_d symmetry [50,51].

The adsorption of a metal halide by the solid phase depends on how MCl_z is associated in the solution phase and on the affinity for this species for the sorbent. In order to have a better understanding of the mechanism of adsorption, equilibrium constants have been determined for the above reaction for some metal halides in ethanol solutions.

The adsorption of MCl_z complex by a solid matrix can be described formally as a reaction between a sorbate entity S and an active sorption center \bar{Q} , where the bar means the solid phase:



where S is MCl_z , \bar{SQ} is the fixed complex, and β is the heterogeneous stability constant. One center may contain several attached groups $-R^+Cl^-$. When complexes of \bar{SQ} of only one type are formed, all sorption centers \bar{Q} are energetically homogeneous and lateral interactions are negligible. The adsorption is of an ideal character and may be described by the Langmuir equation [52]

$$[\bar{SQ}] = t_Q \frac{\beta[S]}{1 + \beta[S]} \quad (3)$$

where $[\bar{SQ}]$ and $[S]$ are the specific concentrations of the adsorbed species and in the solution phase, respectively. From the linearized equation

$$\frac{[S]}{[SQ]} = \frac{1}{\beta t_Q} + \frac{1}{t_Q} [S] \quad (4)$$

by plotting $\frac{[S]}{[SQ]}$ against $[S]$, β , and t_Q are determined.

Deviations from linearity of the plot indicate the non-applicability of the Langmuir equation, normally observed because of the non-ideal character of the adsorption. Among several possible models, one which considers the various pendant functional groups as an assemblage of fixed polydentate centers has been used, since it fits the experimental data properly [53–55]. Calculations of stability constants for several metal halides, for the reaction of eq. 1, have been carried out. The results are summarized in Table 5.

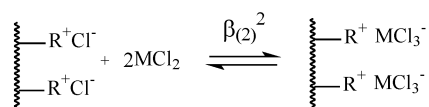
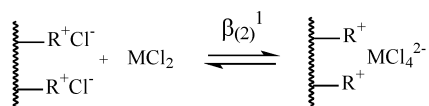
Table 5 Stability constants for metal chlorides chemisorption, from ethanol solutions by cationic functional groups at 298 K.

SiPy ⁺ Cl ⁻ [56]	t_Q , mmol g ⁻¹	$\log \beta_{(2)}^1$	$\log \beta_{(2)}^2$		
CuCl ₂	0.27	3.14 (0.03)	5.20 (0.07)		
		$\log \beta_4^1$	$\log \beta_4^2$	$\log \beta_4^3$	$\log \beta_4^4$
FeCl ₃	0.83	3.66 (0.13)	6.69 (0.10)	a	12.81 (0.10)
ZnCl ₂	0.53	2.63 (0.02)	a	a	10.23 (0.06)
CdCl ₂	0.74	2.41 (0.03)	a	a	10.39 (0.06)
HgCl ₂	0.77	2.79 (0.13)	5.35 (0.32)	a	10.96 (0.20)
SiO ₂ /SiPy ⁺ Cl ⁻ [49]	t_Q , mmol g ⁻¹	$\log \beta_{(1)}^1$			
FeCl ₃	0.60 (0.02)	3.30 (0.06)			
		$\log \beta_{(2)}^1$			
CuCl ₂	0.27 (0.02)	3.19 (0.08)			
ZnCl ₂	0.23 (0.01)	3.58 (0.04)			
PDMS/SiPy ⁺ Cl ⁻ [57]	t_Q , mmol g ⁻¹	$\log \beta_{(1)}$			
CoCl ₂	0.29 (0.01)	3.48 (0.03)			
CuCl ₂	0.31(0.01)	3.98 (0.01)			
		$\log \beta_{(2)}^1$	$\log \beta_{(2)}^2$		
FeCl ₃	0.46 (0.08)	2.69 (0.18)	7.12 (0.02)		
CeI/Al/SiDb ⁺ Cl ⁻ [31]	t_Q , mmol g ⁻¹	$\log \beta_{(1)}^1$			
FeCl ₃	1.42 (0.11)	3.14 (0.14)			
		$\log \beta_{(2)}^1$			
CoCl ₂	0.20 (0.01)	4.08 (0.25)			
CuCl ₂	0.115 (0.005)	3.3 (0.3)			

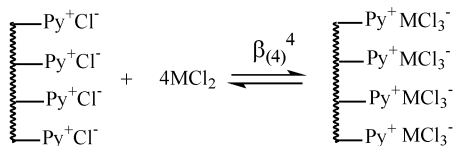
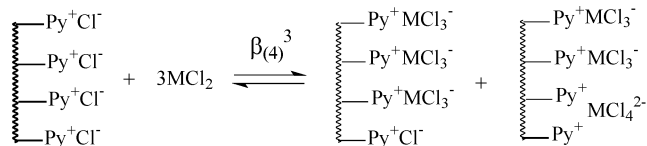
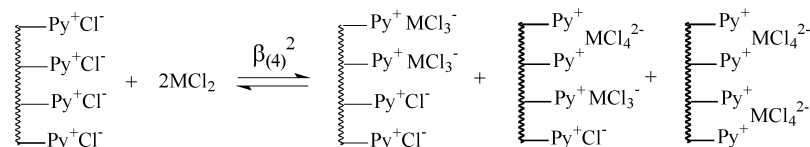
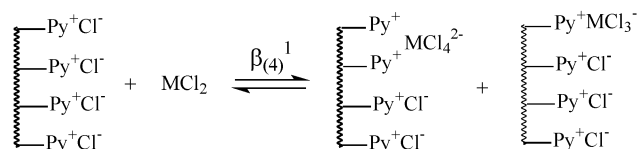
The values in parentheses are the standard deviations.

^aNot determinable.

In Table 5, the constants $\beta_{(n)}^i$ are the stability constant of the reaction described in eq. 1, where n is the assemblage of attached ligands on the surface which act as a mono-, bi-, ... , multidentate fixed center, and t_Q is the specific concentration of active sorption centers. Taking as a particular case of adsorption of MCl_2 by the solid sorbent $SiPy^+Cl^-$, the equilibrium constants can be written as shown in Scheme 5 [56]:



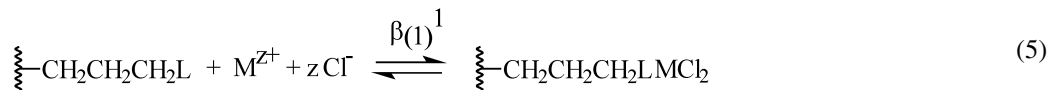
bidentate centers



tetradentate centers

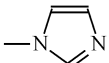
Scheme 5 Representation of MCl_2 interaction with $SiPy^+Cl^-$ material by the model of fixed bidentate and tetradentate centers. Species at the right side of equation are stoichiometrically indistinguishable for the fixed tetradentate centers.

Sorption capacities and stability constants of $\text{CeI}/\text{Al}_2\text{O}_3/\text{Si}(\text{CH}_2)_3\text{L}$ ($\text{L} = -\text{NH}_2$, $-\text{NH}(\text{CH}_2)_3\text{NH}_2$, $-\text{NH}(\text{CH}_2)_3\text{NH}(\text{CH}_2)_3\text{NH}_2$, and imidazole) toward CuCl_2 , ZnCl_2 , and FeCl_3 in ethanol solution are presented in Table 6 [58]. In every case, the interaction of metal halide with the surface-attached ligand is with a monodentate center. The equilibrium reaction in this case is formally expressed as



In this case, the metal halide is also adsorbed as a neutral species, i.e., when the metal ion diffuses into the solid–solution interface, it is followed by the anion.

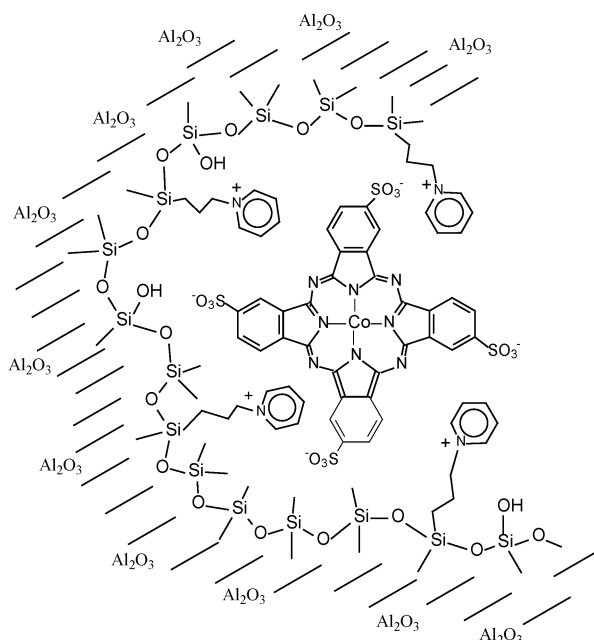
Table 6 Sorption capacities of $\text{CeI}/\text{Al}_2\text{O}_3/\text{Si}(\text{CH}_2)_3\text{L}$, t_{Q} (mmol g^{-1}) and stability constants $\log \beta_{(1)}^1$.

L	CuCl_2		ZnCl_2		FeCl_3	
	t_{Q}	$\log \beta_{(1)}^1$	t_{Q}	$\log \beta_{(1)}^1$	t_{Q}	$\log \beta_{(1)}^1$
$-\text{NH}_2$	0.20 (0.01)	2.98 (0.05)	0.10 (0.003)	4.38 (0.11)	0.22 (0.02)	3.10 (0.13)
$-\text{NH}(\text{CH}_2)_3\text{NH}_2$	0.35 (0.01)	3.38 (0.07)	0.36 (0.02)	3.62 (0.14)	0.79 (0.04)	2.78 (0.07)
$-\text{NH}(\text{CH}_2)_3\text{NH}(\text{CH}_2)_3\text{NH}_2$	0.24 (0.003)	4.43 (0.04)	0.25 (0.01)	4.01 (0.08)	0.75 (0.10)	2.64 (0.13)
	0.24 (0.01)	2.86 (0.06)	0.14 (0.05)	3.22 (0.07)	0.34 (0.03)	2.88 (0.09)

Electrochemical sensors

Substrates S [$\text{S} = \text{SiO}_2$, $\text{SiO}_2/\text{Al}_2\text{O}_3$, Al_2O_3 , cellulose/ Al_2O_3 , C-graphite, and AlPO (aluminum phosphate)] coated with a thin film of SiPy^+Cl^- can be used as support to strongly immobilize electroactive species such as metalated tetrasulfophthalocyanine or metalated porphyrins aiming to prepare electrochemical sensors. Another use of these materials has been the preparation of potentiometric sensors.

To prepare an electrode, an electroactive species is adsorbed on the substrate modified with a functional group able to retain the electroactive species. Scheme 6 illustrates SiPy^+Cl^- adhering to the Al_2O_3 pores on the surface of the matrix and how an electroactive species, the cobalt complex, is retained. Preliminary tests have shown that the complex is not leached from the electrode surface prepared, thus even after long oxidation–reduction cycles using cyclic voltammetry technique.



Scheme 6 Schematic representation of CoTsPc^{4-} immobilized on $\text{Al}_2\text{O}_3/\text{SiPy}^+\text{Cl}^-$ surface.

Figure 10 shows the cyclic voltammograms obtained for oxalic acid oxidation mediated by the cobalt complex. The concentration of oxalic acid was varied between 10^{-3} to 10^{-2} mol l^{-1} and the plot (inset of Fig. 10) of j vs. [oxalic acid] shows a linear correlation within the concentration used to illustrate the electrocatalytic oxidation ability of the electrode [26].

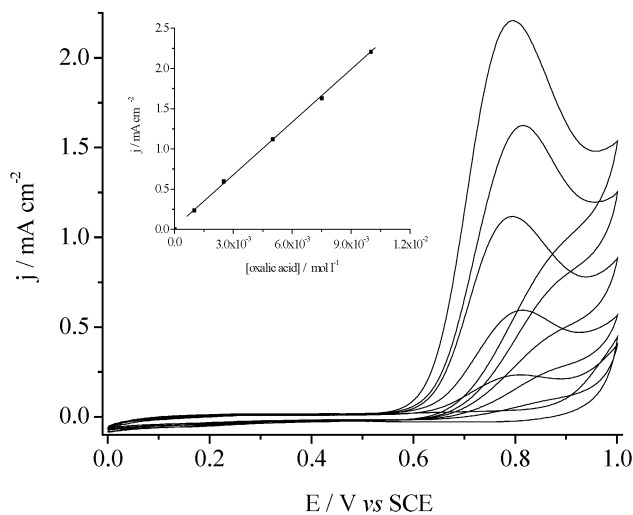


Fig. 10 Cyclic voltammograms obtained for oxalic acid in different concentrations using the $(\text{Al}_2\text{O}_3/\text{SiPy}^+)_4\text{CoTsPc}^{4-}$ carbon paste electrode. Inset figure: Plot of current densities against oxalic acid concentrations. Experimental conditions: scan rate 20 mV s^{-1} , 1 mol l^{-1} KCl (supporting electrolyte solution), pH 4 and 298 K.

Using SiO_2 , $\text{SiO}_2/\text{Al}_2\text{O}_3$, and graphite as substrates to support the thin film of the polymer, electrodes prepared with this material with different immobilized electroactive species have been applied for chemical analyses of oxalic acid in spinach, ascorbic acid in tablets and orange juice, and sacharin in artificial sweeteners. Table 7 summarizes some results obtained by using cyclic voltammetry, chronoamperometry, and potentiometry techniques.

Table 7 Results of chemical analyses using the electrodes, compared to results using standard method of analyses.

Electrodes	Samples	Using the electrodes*	Standard methods
$(\text{SiO}_2/\text{SiPy}^+)_4\text{CoTsPc}^{4-}$ cyclic voltammetry [59]	Oxalic acid in spinach g/100 g of dry sample	s_1 2.22	2.27 [62]
		s_2 0.97	0.98
$(\text{SiO}_2/\text{Al}_2\text{O}_3/\text{SiPy}^+)_4\text{CuTsPc}^{4-}$ chrono amperometry [60]	Ascorbic acid in tablets/g	s_1 1.01	1.038 [63]
		s_2 0.47	0.476
$(\text{Graphite}/\text{SiPy}^+)_4[\text{Fe}(\text{CN})_6]^{4-}$ chrono amperometry [27]	Ascorbic acid in tablets/g	s_1 1.02	1.002 [63]
		s_2 1.04	0.996
	Ascorbic acid in juices g/l	s_1 0.36	0.342 [64]
		s_2 0.25	0.235
Graphite/ $\text{SiPy}^{+/-}$ potentiometry [61]	Sacharin in artificial sweetener (powder) mg/g	s_1 11.6	12.0 [65]
		s_2 25.9	24.8
Graphite/ $\text{SiPy}^{+/-}$ potentiometry [61]	Sacharin in artificial sweetener (liquid) mg/ml	s_1 65.3	68.9 [65]
		s_2 82.0	83.2

* s_1 and s_2 refer to the values found for two different samples.

Tests to determine the potential usefulness of other electrodes prepared with different electroactive species adsorbed on $\text{SiO}_2/\text{PyCl}^-$ have also been made. For instance, FeTsPc has been used to determine dissolved oxygen in water [24], $\text{AlPO}/\text{SiPy}^+/\text{CoTsPc}$ was tested to determine the sensitivity of an electrode prepared with this material toward oxalic acid [29] and $\text{SiO}_2/\text{Al}_2\text{O}_3/\text{FeTsP}$ [where FeTsP is 5,10,15,20-tetrakis-(2,6-difluoro-3-sulfonatophenyl) porphyrinato iron(III)] was tested to determine hydrazine in an aqueous solution [66].

CONCLUSIONS

Silsesquioxanes functionalized with pyridinium and 1,4-diazabicyclo[2.2.2]octane and obtained in a water-soluble form can be used to coat various substrate surfaces as thin films. The matrices obtained in a water-insoluble form [3- and 4-picolinium, 1,4-diazabicyclo[2.2.2]octane (di-cationic group)] can be used directly. The cationic or neutral organofunctional groups have been successfully used to adsorb metal ions from ethanol. PDMS polymer can also be functionalized with neutral amine and pyridinium groups attached to the polymer structure. The stability constants have shown that most of the tested materials have a high affinity for several metals. The particular and interesting characteristics, common to all materials tested, are that they could be easily regenerated, through simple operations, after use. As these materials are, with the exception of the PDMS-modified materials, porous and presenting high specific surface areas, the electroactive species are strongly retained on the matrix surfaces, presumably confined in the pores. Despite this confinement, electrodes made with these porous materials as sub-

strates did not present any significant barrier to diffusion of species on the electrode surfaces in the redox processes. The materials prepared were chemically very stable, even in the case where functionalized silsesquioxane polymers were dispersed on the substrate surfaces, since in this case they are bonded to the matrices by Si–O–SiR or Al–O–SiR chemical bonds. In the case of adhesion on a graphite surface, even though it is presumed that the adhesion is only due to electrostatic interactions, the polymer used, SiPy⁺Cl⁻, also was shown to be strongly adhered.

ACKNOWLEDGMENT

The authors are indebted to Prof. Carol H. Collins for manuscript revision.

REFERENCES

1. P. Tien, L.-K. Chau, Y.-Y. Shieh, W.-C. Lin, G.-T. Wei. *Chem. Mater.* **13**, 1124 (2001).
2. C.-L. Lin, P. Tien, L.-K. Chau. *Electrochim. Acta* **49**, 573 (2004).
3. B. Lee, H.-J. Im, H. Luo, E. W. Hagaman, S. Dai. *Langmuir* **21**, 5372 (2005).
4. M. Kanungo, M. M. Collinson. *Langmuir* **21**, 827 (2005).
5. T.-A. Lin, G.-Y. Li, L.-K. Chau. *Anal. Chim. Acta* **576**, 117 (2006).
6. L. M. L. A. Auler, C. R. Silva, K. E. Collins, C. H. Collins. *J. Chromatogr., A* **1073**, 147 (2005).
7. H. Qiu, S. Jiang, X. Liu. *J. Chromatogr., A* **1103**, 265 (2006).
8. L. A. Belyakova, A. M. Varvarin, N. V. Roik. *Appl. Surf. Sci.* **253**, 784 (2006).
9. B. Gao, S. He, J. Guo, R. Wang. *Mater. Lett.* **61**, 877 (2007).
10. H. Touzi, N. Sakly, R. Kalfat, H. Sfihi, N. Jaffrezic-Renault, M. B. Rammah, H. Zarrouk. *Sens. Actuators, B* **96**, 399 (2003).
11. C.-L. Lin, P. Tien, L.-K. Cha. *Electrochim. Acta* **49**, 573 (2004).
12. A. A. Muxel, D. A. Jesus, R. V. S. Alfaya, A. A. S. Alfaya. *J. Braz. Chem. Soc.* **18**, 572 (2007).
13. E. M. Wong, M. A. Markowitz, S. B. Quadri, S. L. Golledge, D. G. Castner, B. P. Gaber. *Langmuir* **18**, 972 (2002).
14. B. Lee, L.-L. Bao, H.-J. Im, S. Dai, E. W. Hagaman, J. S. Lin. *Langmuir* **19**, 4246 (2003).
15. C. Wu, T. Xu, W. Yang. *Eur. Polym. J.* **41**, 1901 (2005).
16. J. C. Moreira, Y. Gushikem. *J. Colloid Interface Sci.* **107**, 70 (1985).
17. J. C. Moreira, Y. Gushikem. *Anal. Chim. Acta* **176**, 263 (1985).
18. M. S. Iamamoto, Y. Gushikem. *Analyst* **114**, 983 (1989).
19. A. M. Lazzarin, R. Landers, Y. V. Kholin, Y. Gushikem. *J. Colloid Interface Sci.* **254**, 31 (2002).
20. N. L. Dias Filho, F. Marangoni, R. M. Costa. *J. Colloid Interface Sci.* **313**, 34 (2007).
21. Brazilian National Petroleum Agency web site. Norm 36. In <<http://www.anp.gov.br>> Access in Jul 01, 2007.
22. Y. Gushikem, R. V. S. Alfaya, A. A. S. Alfaya. Preparation process of 3-*n*-propylpyridinium-silsesquioxane bonded to a silsesquioxane structure. Patent INPI No. PI9803053-1 (1998).
23. L. T. Arenas, A. Langard, Y. Gushikem, C. C. Moro, E. V. Benvenutti, T. M. H. Costa. *J. Sol-Gel Sci. Technol.* **28**, 51 (2003).
24. E. S. Ribeiro, Y. Gushikem. *Electrochim. Acta* **44**, 3589 (1999).
25. S. T. Fujiwara, Y. Gushikem, R. V. S. Alfaya. *Colloids Surf., A* **178**, 135 (2001).
26. A. M. S. Lucho, F. L. Pissetti, Y. Gushikem. *J. Colloid Interface Sci.* **275**, 251 (2004).
27. R. V. S. Alfaya, Y. Gushikem, A. S. Alfaya, Y. Gushikem. *J. Braz. Chem. Soc.* **11**, 281 (2000).
28. R. V. S. Alfaya, Y. Gushikem. *J. Colloid Interface Sci.* **213**, 438 (1999).
29. A. M. S. Lucho, E. C. Oliveira, H. O. Pastore, Y. Gushikem. *J. Electroanal. Chem.* **573**, 55 (2004).
30. L. T. Arenas, T. A. S. Aguirre, A. Langaro, Y. Gushikem, E. V. Benvenutti, T. M. H. Costa. *Polymer* **44**, 5521 (2003).
31. G. Splendorea, E. V. Benvenutti, Y. V. Kholin, Y. Gushikem. *J. Braz. Chem. Soc.* **16**, 147 (2005).

32. W. E. Stone, G. M. S. El-Shafei, J. Sanz, S. A. Sellim. *J. Phys. Chem.* **97**, 10127 (1993).
33. B. S. Lartiges, J. Y. Bottero, L. S. Derendinger, B. Humbert, P. Tekely, H. Suty. *Langmuir* **13**, 147 (1997).
34. T. Xu, N. Kob, R. S. Drago, J. B. Nicholas, J. F. Haw. *J. Am. Chem. Soc.* **119**, 12231 (1997).
35. H. A. Magosso, A. V. Panteleimonov, Y. V. Kholin, Y. Gushikem. *J. Colloid Interface Sci.* **303**, 18 (2006).
36. L. T. Arenas, S. L. P. Dias, C. C. Moro, T. M. H. Costa, E. V. Benvenutti, A. M. S. Lucho, Y. Gushikem. *J. Colloid Interface Sci.* **297**, 244 (2006).
37. K. J. Shea, D. A. Loy. *Chem. Mater.* **13**, 3306 (2001).
38. H. Muramatsu, R. J. P. Corriu, B. Boury. *J. Am. Chem. Soc.* **125**, 854 (2003).
39. B. Boury, F. Ben, R. J. P. Corriu, P. Delord, M. Nobili. *Chem. Mater.* **14**, 730 (2002).
40. M. P. Kapoor, Q. Yang, I. Shinji. *Chem. Mater.* **16**, 1209 (2004).
41. S. U. A. Redondo, E. Radovanovic, I. L. Torriani, I. V. P. Yoshida. *Polymer* **42**, 1319 (2000).
42. A. González-Campo, B. Boury, F. Teixidor, R. Núnñez. *Chem. Mater.* **18**, 4344 (2006).
43. F. L. Pissetti, Y. Gushikem. Unpublished results.
44. M. S. Yamamoto, Y. Gushikem. *J. Colloid Interface Sci.* **129**, 162 (1989).
45. P. Tundo, P. Venturello, E. Angeletti. *J. Am. Chem. Soc.* **104**, 6547 (1982).
46. Y. Gushikem, W. C. Moreira. *Colloids Surf.* **25**, 155 (1987).
47. L. T. Arenas, N. M. Simon, Y. Gushikem, T. M. H. Costa, E. C. Lima, E. V. Benvenutti. *Eclat. Quim.* **31**, 53 (2006).
48. L. T. Arenas, E. C. Lima, A. A. dos Santos, J. C. P. Vagheti, T. M. H. Costa, E. V. Benvenutti. *Colloids Surf., A* **297**, 240 (2007).
49. R. V. S. Alfaya, S. T. Fujiwara, Y. Gushikem, Y. V. Kholin. *J. Colloid Interface Sci.* **269**, 32 (2004).
50. K. Nakamoto. *Infrared and Raman Spectra of Inorganic and Coordination Compounds, Part A, Theory and Applications in Inorganic Chemistry*, p. 193, John Wiley, New York (1997).
51. J. S. Avery, C. D. Burbridge, D. M. Goodgame. *Spectrochim. Acta, Part A* **24**, 1721 (1968).
52. I. Langmuir. *J. Am. Chem. Soc.* **40**, 1361 (1918).
53. U. P. Strauss, B. W. Barbieri, G. Wong. *J. Phys. Chem.* **83**, 2840 (1979).
54. U. P. Strauss. *Macromolecules* **15**, 1567 (1982).
55. G. V. Kudryavtsev, D. V. Milchenko, V. V. Yagov, A. A. Lopatkin. *J. Colloid Interface Sci.* **140**, 114 (1990).
56. A. M. S. Lucho, A. Panteleimonov, Y. V. Kholin, Y. Gushikem. *J. Colloid Interface Sci.* **310**, 47 (2007).
57. F. L. Pissetti, H. A. Magosso, I. V. P. Yoshida, Y. Gushikem, S. O. Myernyi, Y. V. Kholin. *J. Colloid Interface Sci.* **314**, 38 (2007).
58. A. M. Lazarin, R. Landers, Y. V. Kholin, Y. Gushikem. *J. Colloid Interface Sci.* **254**, 31 (2002).
59. E. S. Ribeiro, Y. Gushikem. *Electroanalysis* **11**, 1280 (1999).
60. S. T. Fujiwara, C. A. Pessoa, Y. Gushikem. *Anal. Lett.* **35**, 1117 (2002).
61. R. V. S. Alfaya, A. A. S. Alfaya, Y. Gushikem, S. Rath, F. G. R. Reyes. *Anal. Lett.* **33**, 2859 (2000).
62. W. Riemenschneider, M. Tanifuji. *Ullman's Encyclopedia of Industrial Chemistry*, VCH, Weinheim, **A18**, 247 (1998).
63. M. I. Karayannis. *Anal. Chim. Acta* **76**, 121 (1975).
64. J. Lindquist. *Analyst* **100**, 339 (1975).
65. J. F. Lawrence, C. F. Charbonneau. *J. AOAC Int.* **71**, 934 (1988).
66. S. T. Fujiwara, Y. Gushikem, C. A. Pessoa, S. Nakagaki. *Electroanalysis* **17**, 783 (2005).